Optical steering of high and low index microparticles by manipulating an off-axis optical vortex

2005 J. Opt. A: Pure Appl. Opt. 7 1

(http://iopscience.iop.org/1464-4258/7/1/001)

INSTITUTE OF PHYSICS PUBLISHING JOURNAL OF OPTICS A: PURE AND APPLIED OPTICS

J. Opt. A: Pure Appl. Opt. **7** (2005) 1–6 doi:10.1088/1464-4258/7/1/001

Optical steering of high and low index microparticles by manipulating an off-axis optical vortex

W M Lee[1], B P S Ahluwalia[1], X-C Yuan[1,3], W C Cheong[1] and K Dholakia[2]

[1] Photonics Research Centre, School of Electrical and Electronic Engineering, Nanyang Technological University, Nanyang Avenue, 639798, Singapore
[2] School of Physics and Astronomy, University of St Andrews, Fife KY16 9SS, UK

E-mail: excyuan@ntu.edu.sg

Received 17 August 2004, accepted for publication 8 November 2004
Published 19 November 2004
Online at stacks.iop.org/JOptA/7/1

Abstract
We demonstrate the use of a rotating off-axis optical phase singularity, generated through an intentional misalignment of a high optical efficiency spiral phase plate (SPP), to optically steer both high and low index microparticles trapped within the optical beam in a controlled manner. This intentional misalignment of the SPP creates an asymmetrical intensity beam pattern due to the optical vortex being displaced from the centre of the beam propagation axis. By using this optical beam pattern, we propose that a cell can be trapped by an optical beam of matching beam diameter while its internal structure can be manipulated by the off-axis optical vortex.

Keywords: beam shaping, beam splitting, optical elements, devices and systems, beam characteristics, spatial pattern formation

M This article features online multimedia enhancements

(Some figures in this article are in colour only in the electronic version)

1. Introduction

A singular optical beam possesses a helical phase wavefront, which contains an azimuthal phase term of the form $e^{il\theta}$ (l is an integer). The resulting behaviour of the Poynting vector means the beam possesses a uniform orbital angular momentum that can be observed through its mechanical torque on a variety of microparticles [1, 2]. The beam centre where the phase is ill-defined appears dark. Thus such singular optical beams exhibit an intensity pattern of the form of an annular ring that can trap [3, 4] and stack high index microparticles around their annular intensity rings [5] and low index microparticles within the annular intensity ring. Furthermore, by collinearly interfering such a singular beam with either its mirror image or a Gaussian beam one can create a pattern of rotating intensity spots that can trap and stack microparticles and further rotate them in a controlled manner [6, 7]. At present, optical trapping work using singular beams employs beams such as Laguerre–Gaussian (LG) light modes [2] and high-order Bessel light modes [1] that have on-axis optical singularities. Such light modes may allow rotation of micro-objects by transfer of orbital angular momentum, by a variety of mechanisms [1, 2]. These new mechanical effects derived from singular optical beams offer an additional degree of freedom with respect to existing optical micromanipulation techniques. On the other hand, studies of an off-axis optical vortex embedded within a Gaussian background intensity distribution have focused on the exhibition of fluid-like vortex motion [8]. More recently, the rotational Doppler effect (RDE) was demonstrated using a rotating prism to rotate the intensity distribution of a Gaussian beam with a single embedded vortex offset from the beam axis [9]. It is therefore well-known that displacing the optical vortex beam away from the beam axis forms a unique asymmetrical beam pattern due to the diffraction. In this paper, we demonstrate the use of this unique beam pattern of the off-

[3] Author to whom any correspondence should be addressed.

axis vortex to trap and rotate both high and low index particle using the high and low intensity regions of the optical beam pattern respectively. A highly efficient spiral phase plate (SPP) is inserted into a standard optical trapping system. The SPP is then intentionally misaligned in a direction orthogonal to the beam propagation direction. This allows for an efficient formation of a stable asymmetrical optical light pattern which is an off-axis vortex beam. We show that, by rotating this highly efficient SPP around the beam axis, rotating off-axis optical vortex beams are formed. Such optical beams are subsequently used for optical rotation and steering of both high and low index particles.

2. Generation of an off-axis optical vortex from a spiral phase plate

The spiral phase plate is generated by electron beam lithography (EBL) direct writing on SU8 negative resist [10]. The spiral phase structure is directly based on the mathematical expression of a helical wavefront of $e^{il\phi}$ [11–14]. By varying the e-beam energy dosages at different parts of the circular area, an SPP is fabricated. An on-axis optical vortex is formed at the centre of the beam axis when the illuminating beam is directed at the central axis of the SPP. The SPP induces a helical 2π phase retardation step around the central axis of the input optical beam, thus changing the phase of the input optical beam. This change of phase causes a formation of an optical vortex at the central axis of the optical beam [10]. It is important to note that the output helical beam from an SPP is not a pure Laguerre–Gaussian mode but rather a superposition of different Laguerre–Gaussian modes [12].

To mathematically understand this process, we choose a complex Gaussian amplitude as the input beam propagating through the SPP. This is consistent with our experiment in the later section as we make use of a TEM_{00} mode beam as the input optical beam. By inserting the phase element along the propagation axis of the optical beam with complex Gaussian amplitude, the output optical beam will consist of the complex Gaussian amplitude multiplied by the helical phase term of the form of $e^{il\phi}$. The amplitude of the light field may then be expressed in cylindrical coordinates as

$$E(r,\phi,z) = \exp\left(\frac{-r^2}{w^2(z)}\right) \times \exp\left\{-\mathrm{i}\left(\frac{kr^2 z}{2(z^2+z_\mathrm{R}^2)} + \tan^{-1}\frac{z}{z_\mathrm{R}}\right)\right\}\exp(\mathrm{i}l\phi) \qquad (1)$$

where $r = \sqrt{x^2+y^2}$, $\phi = \arctan(\frac{y}{x})$, l is the number of cycles of 2π phase around the optical beam circumference, k is the wavenumber and $w(z)$ is the radius of the beam waist at the propagation distance z, z_R is the Rayleigh range.

Therefore by displacing the SPP orthogonally to the input optical beam propagation direction, a localized 2π phase retardation can be generated at different portions of the beam thus forming an off-axis optical vortex. By introducing an intentional transverse misalignment of the SPP with the illumination optical beam, we are in fact displacing the helical phase function about the beam axis, thus shifting the vortex point as shown in figure 1. The mathematical expression of an off-axis optical vortex beam may be modified from equation (1) which is then given by

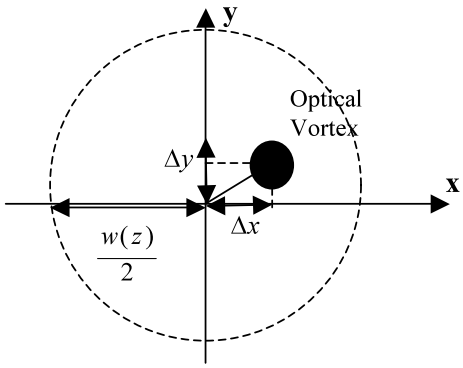

Figure 1. The dark spot shows the position of the optical singularity being displaced $(\Delta x, \Delta y)$ from the centre of the beam axis. The external dotted circle shows the beam waist, $\frac{w(z)}{2}$, of the input optical beam at a propagation distance of z.

$$E(r,\phi,z) = \exp\left(\frac{-r^2}{w^2(z)}\right) \times \exp\left\{-\mathrm{i}\left(\frac{kr^2 z}{2(z^2+z_\mathrm{R}^2)} + \tan^{-1}\frac{z}{z_\mathrm{R}}\right)\right\}\exp(\mathrm{i}l\phi^1) \qquad (2)$$

where $r = \sqrt{x^2+y^2}$, $\phi^1 = \arctan(\frac{y\pm\Delta y}{x\pm\Delta x})$, where Δy and Δx are the displacement of the optical vortex away from the beam central axis as shown in figure 1.

It is important to note that the displacement of the optical vortex about the Gaussian beam waist of $w(z)$, radius of the beam waist at the propagation distance z, critically defines the far-field diffracted intensity pattern observed at Rayleigh's range of z_R. Using the scalar diffraction theory, we numerically calculate the intensity distribution of the optical vortex, generated from the SPP, that is transversely displaced greater or lower than $w(z)$ away from the beam central axis, as described in equation (2) and shown in figure 2. In the simulation, we place the SPP at a propagation distance $z = 0$; the output off-axis optical vortex is then propagated to the far-field diffraction distance.

Hence, in figure 2(A), we show that once the optical vortex, generated from an SPP, is being displaced a transverse distance greater than half of the incident optical beam waist, $w(z)$, at a propagation distance $z = 0$, where $\Delta y \geqslant \frac{w(0)}{2}$ and $\Delta x \geqslant \frac{w(0)}{2}$, the far-field intensity distribution will resemble the interference pattern of an LG beam with topological charge one and a Gaussian beam. Therefore, in this case, the intensity variation around the annular ring deviates more than 50% so the optical vortex intensity distribution is no longer maintained, as shown in figure 2(B).

On the other hand, in figure 2(C), it is demonstrated in simulation that once the optical vortex, generated from an SPP, is displaced a transverse distance less than half of the incident optical beam waist, $w(z)$, at a propagation distance $z = 0$, where $\Delta y \leqslant \frac{w(0)}{2}$ and $\Delta x \leqslant \frac{w(0)}{2}$, the optical vortex integrity is still maintained within the optical beam and we obtain a circular beam with an off-axis enclosed intensity null. Hence the intensity variation around the annular ring deviates less than 50%, as shown in figure 2(D).

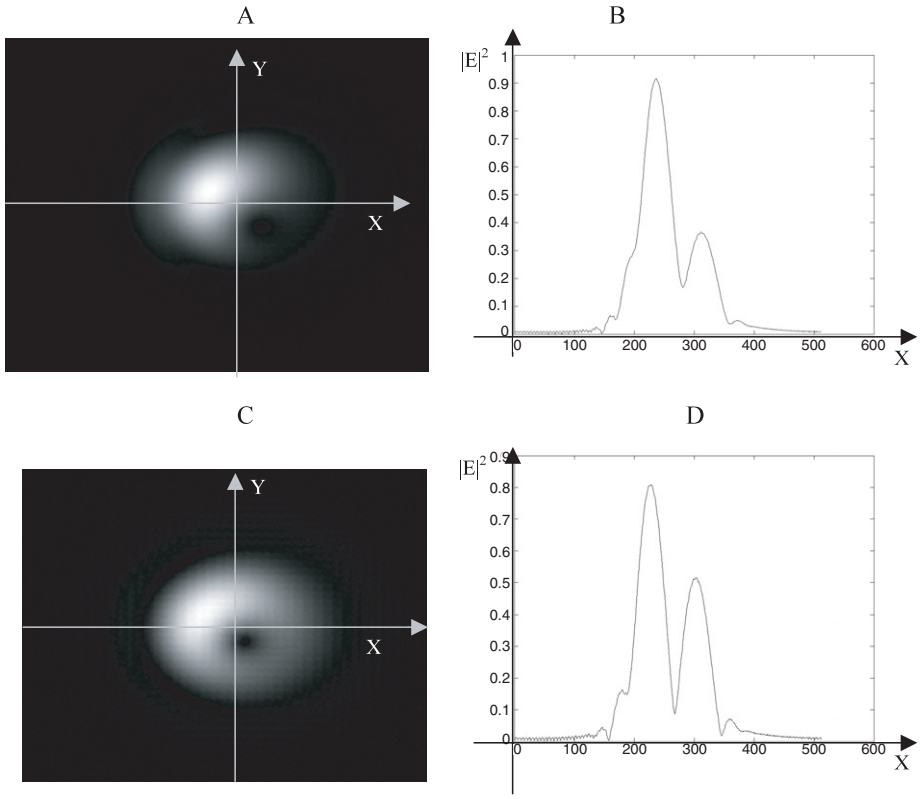

Figure 2. Numerical simulation results of two off-axis optical vortex displacement positions' intensity distributions. Note that the SPP, generating the optical vortex, is numerically displaced away from the beam axis at a propagation distance $z = 0$ and the output off-axis optical vortex due to the displaced SPP is then propagated to the far-field distance. (A) Shows the two-dimensional far-field transverse intensity distribution of the off-axis optical vortex beam, $|E|^2$, when the SPP was displaced at $\frac{3}{2}w(0)$, at a propagation distance of $z = 0$. (B) Shows the far-field cross-sectional transverse intensity distribution of the off-axis optical vortex, $|E|^2$, across the x-axis. (C) Shows the two-dimensional far-field transverse intensity distribution, of the off-axis optical vortex beam, $|E|^2$, when the SPP was displaced at $\frac{2}{3}w(0)$, at a propagation distance of $z = 0$. (D) Shows the far-field cross-sectional transverse intensity distribution of the off-axis optical vortex, $|E|^2$, across the x-axis.

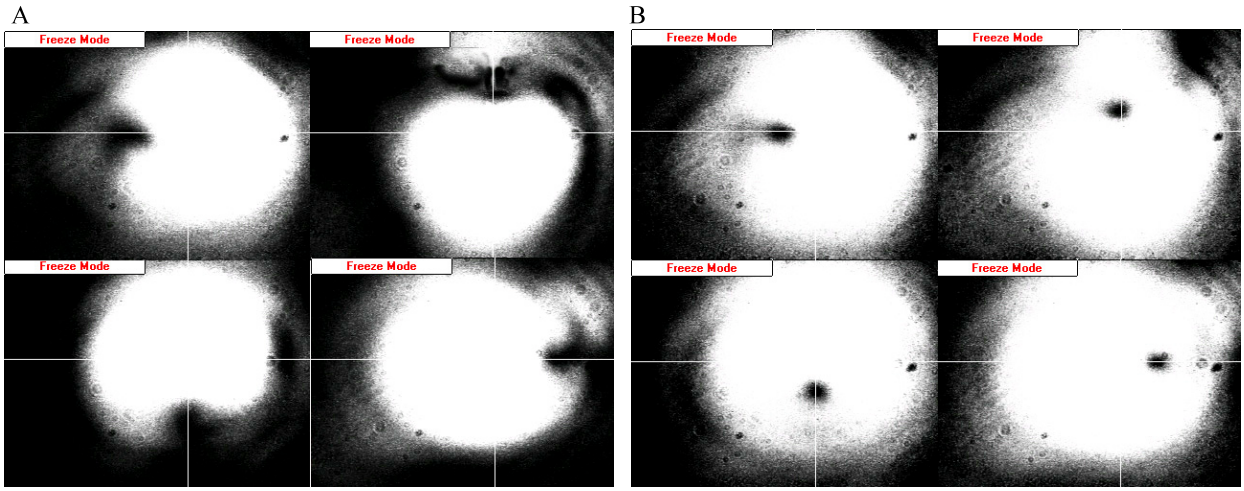

Figure 3. Experimental results of the two sets of asymmetrical intensity patterns where the optical vortex is displaced by a distance greater or smaller than half of $w(z)$ away from the beam axis. (A) By displacing the optical phase singularity a distance greater than $\frac{w(z)}{2}$, the rotating intensity of a C shape is being generated. (B) By displacing the optical singularity a distance smaller than $\frac{w(z)}{2}$, the optical vortex integrity is still present in the beam.The online edition (stacks.iop.org/JOptA/7/1) includes a real-time video of the manipulation of the off-axis optical vortex within a Gaussian beam at the sample plane.

Now if we induce this misalignment and then rotate the SPP around the Gaussian beam propagation direction, we are either creating a rotating optical vortex off-centre from the beam axis [15], shown experimentally in figure 3(A), or an asymmetrical intensity pattern that resembles an interference pattern of an LG with charge one and a Gaussian beam [9],

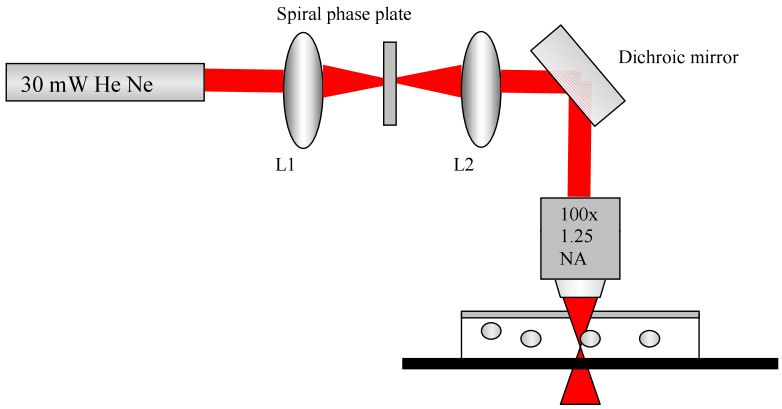

Figure 4. In the set-up, a 30 mW linearly polarized HeNe laser with a low Gaussian beam divergence angle is collimated into the 100× microscopic objective of NA 1.25 for trapping using the telescopic arrangement using lenses L1 and L2. The SPP, of 500 μm in diameter, is inserted in between the pair of lenses L1 and L2, and is mounted on a rotating x–y–z stage.

shown experimentally in figure 3(B), in this instance in a more straightforward manner than previously realized [6]. It is these asymmetric intensity patterns that are subsequently used to trap and rotate high and low index microspheres respectively.

Blazed computer-generated holograms (CGH) are typically the method of choice when creating singular optical beams for optical trapping [1–4]; however, they generate light modes in their first diffracted order thus causing a deviation in the beam propagation path. The key advantages of using the micron-sized SPP to generate an optical vortex beam are that they are more efficient, induce no beam deviation and are compact enough to be inserted and removed from the beam path in an optical tweezers set-up with little or no loss of alignment [10]. The efficiency of the fabricated SPP used was around 95%. This high optical efficiency exceeds that of other methods of obtaining similar optical traps such as binary holograms of around 40% optical efficiency, a 70% optical efficiency for a blazed hologram or a spatial light modulator of optical efficiency 50% or introducing an aperture within the beam to create an asymmetric profile with an optical efficiency of only 40% [16]. In the next section, we discuss experimental results obtained using our SPP generated asymmetrical optical beam patterns in optical tweezers. Furthermore, we propose that this method may be exploited to optically manipulate intracellular structures.

3. Optical rotation of high and low index particle off-axis optical vortex

In the figure 4, the experimental set-up is presented, where the SPP, with a helical phase step of 2π where $l = 1$, is mounted onto a rotating translation (x–y–z) stage, in the propagation path of the 30 mW linearly polarized HeNe laser of 632.8 nm. The resultant beam is subsequently directed into the epi-fluorescence port of the upright microscope (Carl Zeiss Axiostar plus) and focused with a ×100 microscope objective to a waist size of around 5 μm within a sample chamber within which we dispersed a range of microparticles in water.

The optical trapping of high and low index microparticles occurs by different mechanisms. The term 'high index' denotes an index of refraction of the microparticles higher than that of the surrounding medium and 'low index' lower than that of the surrounding medium. In order for a high index particle to be stably trapped in three dimensions, the net optical gradient forces and scattering forces have to be balanced. However, for low index microparticles, the refracted light results in optical forces that repel microparticles away from the most intense part of the light beam. In order for a low index microparticle to be stably held, the net repelling optical forces may cage the microparticles at an intensity minimum [3]. Hence, an optical vortex beam with an annular intensity ring is utilized to trap these low index microparticles at its null intensity point at the beam centre [3, 4]. We show controlled rotation and steering of both high and low index particles utilizing the two sets of asymmetrical intensity pattern shown in figures 3(A) and (B).

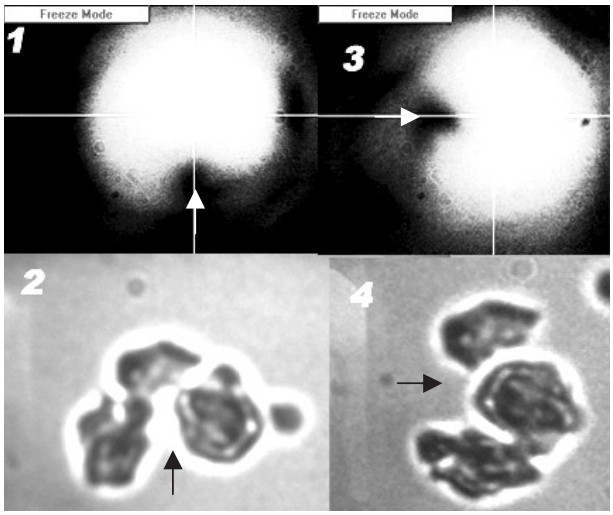

Figure 5. Three calcite particles of size 3–5 μm are being trapped at two different orientations of a C-shaped intensity pattern (figure 3(A)) due to the off-axis optical vortex, in frames 1 and 3. Frames 2 and 4 show the corresponding calcite particles being trapped in the intensity pattern. The black and white arrows mark the opening at the C-shape intensity corresponding to the arrangement of the trapped calcite.

First, to validate the asymmetrical intensity distribution due to the off-axis optical vortex hosted within the Gaussian beam, we managed to trap three irregularly shaped calcite particles of around 3–5 μm in size, at two different positions of the off-axis optical vortex beam, as shown in figure 5. As expected, this amalgamation of particles follows the imposed

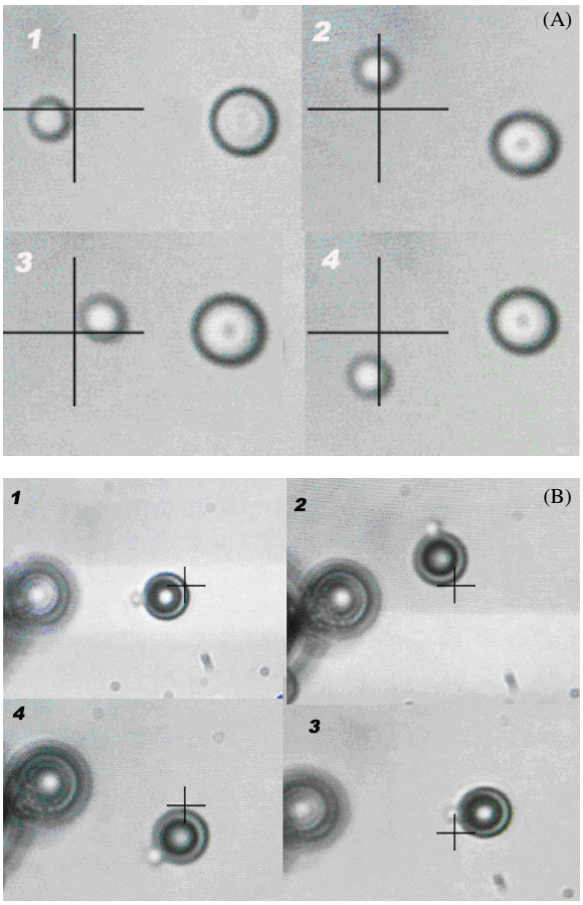

Figure 6. The controlled rotation of both high and low index microparticles using the two sets of intensity patterns shown in figures 2(A) and (B) suspended in deionized water. (A) High index silica microspheres ($n = 1.59$) of 3 μm being trapped and rotated by asymmetrical intensity distribution from a misaligned SPP as shown in figure 2(A). (B) Hollow microspheres (shell thickness of 5–10% of their total diameter) of 5 μm being trapped and rotated by the rotating optical vortex from a misaligned SPP as shown in figure 2(B).

and rotated intensity distribution. In this case, the SPP is being displaced at more the half the beam waist from its central symmetrical position, away from the beam's central axis as in figure 3(A). In figure 6(A), a single high index silica microsphere is rotated around the beam axis, as indicated by the cross. The rotation of the sphere is clockwise, identical to the rotation direction of the asymmetrical intensity pattern as shown in figure 3(A).

We then adjusted the SPP to yield a light beam as in figure 3(B). Using this pattern, a single hollow sphere microsphere is trapped and rotated around the beam axis as indicated by the cross (see figure 6(B)). This rotation is due to the rotating optical vortex around the beam axis. This is the first controlled low index particle rotation by a rotational asymmetrical beam profile (rotating null intensity point) to the best of our knowledge.

A key advantage in manipulating particles around the beam axis is the ability to manipulate particles within a cellular structure. After trapping a large cellular structure using an optical beam of matching beam waist, we may manipulate the internal structure of the cell by simply displacing the vortex position with respect to the beam axis and subsequently rotating the SPP. Displacing the optical vortex from the beam axis may allow a relative strong trapping of the cell whilst at the same time optically steering the internal cellular structure.

In figure 7, we show a pseudo-cellular structure where a vesicle is filled with a mixture of small microspheres beside a Gaussian beam of matching beam diameter of around 10 μm in diameter. By employing the intensity pattern from the off-axis optical vortex shown in figure 3(B), the vesicle can be easily rotated around its own axis in a controlled clockwise direction. This rotation is due to the manipulation of the high and low index microspheres within the vesicle. This optical rotation is occurring while the vesicle is being trapped by the annular intensity optical beam imposed by the intensity pattern shown in figure 3(B). However, in the experimental result, we observed that the rotating high and low microparticles in the pseudo-cellular structure also caused the entire cellular

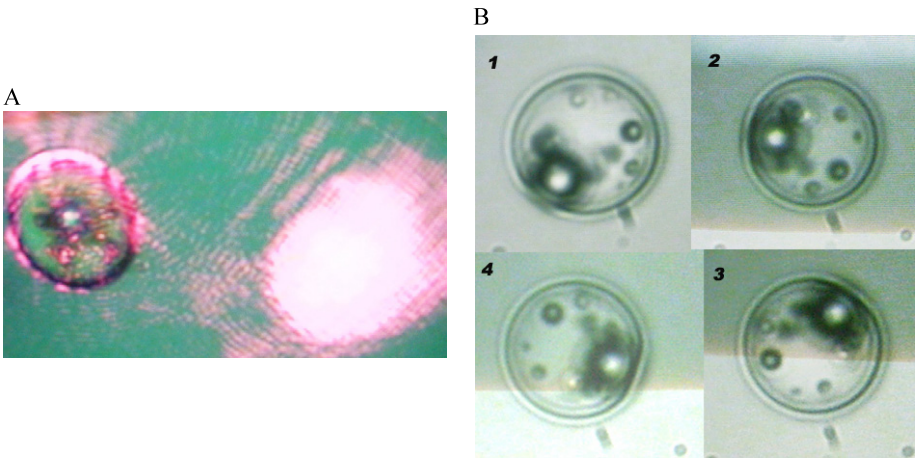

Figure 7. A vesicle being inserted with microspheres to simulate a pseudo-cellular structure environment. This demonstrates that the set of asymmetrical intensity patterns shown in figures 2(A) and (B) can perform controlled rotation of the internal sections of a cellular structure without further focusing of the spot size of the trapping beam by just using the off-axis optical vortex beam. (A) The size of the pseudo-cellular structure matches that of the beam diameter of the trapping optical beam. (B) There is a 3 μm-size microsphere being manipulated which is rotating the entire vesicle.

structure to rotate as well. This is believed to be due to the strong adhesive force that the internal microspheres have on the surface of the wall of the pseudo-cellular structure. This therefore shows that rotating the off-axis optical vortex around from the beam axis allows the microparticle to overcome the drag force given by Stokes law,

$$\tau_{\mathrm{v}} = -8\pi\eta r^3 w, \tag{3}$$

where η is the viscosity of the surroundings, r is the radius of the particle and w is the angular velocity of the particle due to the rotating off-axis optical vortex trap.

These experimental results demonstrate that by steering the position of the optical vortex within a Gaussian beam, by displacement of the SPP in the optical trapping beam path, both high and low index microparticles can be steered or potentially rotated even within a vesicle.

4. Conclusion

In conclusion, we have explored off-axis optical vortex beams as candidates for optical steering and rotation of microparticles. By displacing an SPP we can create beams that can controllably rotate both high and low index particles. We were able to demonstrate for the first time controlled optical rotation of low-index microparticles around the trapping beam axis.

We note that we did not investigate the orbital angular momentum from the inclined wavefront in the off-axis optical vortex beam [17, 18] due to the fact that the available laser power was low and particle rotation due to scattering of light was observed to be too slow and inconclusive. However, future studies on the orbital angular momentum of the light with respect to the vortex position within the beam will be dealt with in detail with a higher power laser.

Our experiment shows the simplicity and versatility of a single SPP incorporated into an optical trapping system. It allows a wide range of optical manipulation to be performed, particularly the controlled rotation of a low-index particle [1, 6] around the beam axis.

Acknowledgment

This work is supported by the Agency for Science, Technology and Research (A*STAR) of Singapore under A*STAR SERC Grant No. 032 101 0025.

References

[1] Garcés-Chávez V, Volke-Sepulveda K, Chávez-Cerda S, Sibbett W and Dholakia K 2002 Transfer of orbital angular momentum to an optically trapped low-index particle *Phys. Rev.* A **66** 063402

[2] He H, Friese M E J, Heckenberg N R and Rubinsztein-Dunlop H 1995 Direct observation of transfer of angular-momentum to absorptive particles from a laser-beam with a phase singularity *Phys. Rev. Lett.* **75** 826

[3] Gahagan K T and Swartzlander G A Jr 1999 Optical vortex trapping of particles *Opt. Lett.* **21** 827

[4] Gahagan K T and Swartzlander G A 1999 Simultaneous trapping of low-index and high-index microparticles observed with an optical-vortex trap *J. Opt. Soc. Am.* B **16** 533

[5] Lee W M and Yuan X-C 2003 Observation of three-dimensional optical stacking of microparticles using a single Laguerre–Gaussian beam *Appl. Phys. Lett.* **83** 5124

[6] Paterson L, MacDonald M P, Arlt J, Sibbett W, Bryant P E and Dholakia K 2001 Controlled rotation of optically trapped microscopic particles *Science* **292** 912

[7] MacDonald M P, Paterson L, Volke-Sepulveda K, Arlt J, Sibbett W and Dholakia K 2002 Creation and manipulation of three-dimensional optically trapped structures *Science* **296** 1101

[8] Rozas D, Law C T and Swartzlander G A Jr 1997 Propagation dynamics of optical vortices *J. Opt. Soc. Am.* B **14** 3054
Rozas D, Sacks Z S and Swartzlander G A Jr 1997 Experimental observation of fluidlike motion of optical vortices *Phys. Rev. Lett.* **79** 3399

[9] Basistiy I V, Slyusar V V, Soskin M S, Vasnetsov M V and Bekshaev A Ya 2004 Manifestation of the rotational Doppler effect by use of an off-axis optical vortex beam *Opt. Lett.* **28** 1185

[10] Cheong W C, Lee W M, Yuan X-C, Dholakia K, Zhang L S and Wang H 2004 Direct electron beam writing of continuous spiral phase plates in SU-8 with high power efficiency for optical manipulation *Appl. Phys. Lett.* at press

[11] Turnbull G A, Robertson D A, Smith G M, Allen L and Padgett M J 1996 The generation of free-space Laguerre–Gaussian modes at millimetre-wave frequencies by use of a spiral phaseplate *Opt. Commun.* **127** 183

[12] Beijersbergen M W, Coerwinkel R P C, Kristensen M and Woerdman J P 1994 Helical-wavefront laser beams produced with a spiral phaseplate *Opt. Commun.* **112** 321

[13] Oemrawsingh S S R, van Houwelingen J A W, Eliel E R, Woerdman J P, Verstegen J K, Kloosterboer J G and 'tHooft G W 2004 Production and characterization of spiral phase plates for optical wavelengths *Appl. Opt.* **43** 688

[14] Ganic D, Gan X, Gu M, Hain M, Somalingam S, Stankiovic S and Tschudi T 2002 Generation of doughnut laser beam by use of liquid-crystal cell with a conversion efficiency near 100% *Opt. Lett.* **27** 1351

[15] Swartzlander G A Jr 1999 Optical vortex filament *Horizons in World Physics* vol 228 (New York: Nova Science) p 107

[16] O'Neil A T and Padgett M J 2002 Rotational control within optical tweezers by use of a rotating aperture *Opt. Lett.* **27** 743

[17] Allen L, Beijersbergen M W, Spreeuw R J C and Woerdman J P 1992 Orbital angular momentum of light and the transformation of Laguerre–Gaussian laser modes *Phys. Rev.* A **45** 8185

[18] Roux F S 2004 Distribution of angular momentum and vortex morphology in optical beams *Opt. Commun.* **242** 45